

# Translational Diffusion of Ion Radicals Created by Electron Transfer in Charged Micellar Solutions Probed by the Transient Grating Method and the Taylor Dispersion Method

Koichi Okamoto,<sup>†,‡</sup> Noboru Hirota,<sup>‡</sup> Toshihiro Tominaga,<sup>§</sup> and Masahide Terazima<sup>\*,‡</sup>

Department of Chemistry, Graduate School of Science, Kyoto University, Kyoto, 606-8502 Japan, and  
Department of Applied Chemistry, Okayama University of Science, 1-1 Ridai-cho, Okayama, 700-0005, Japan

Received: December 20, 2000; In Final Form: April 9, 2001

Diffusion processes of intermediate ion radicals created by the photoexcited electron-transfer reaction of benzoquinone (BQ) and aniline (AN) in sodium dodecyl sulfate (SDS; anionic micelle) and cetyltrimethylammonium bromide (CTAB; cationic micelle) solutions were studied by using the transient grating (TG) and Taylor dispersion (TD) methods. The diffusion coefficients ( $D$ ) of the anion radical of BQ ( $BQ^{\bullet-}$ ) in SDS and the cation radical of AN ( $AN^{\bullet+}$ ) in CTAB are similar to  $D$  of those radicals in neat water, while  $D$  of  $AN^{\bullet+}$  in SDS and  $D$  of  $BQ^{\bullet-}$  in CTAB are smaller than  $D$  in neat water and more close to  $D$  of the self-diffusion of the micelles of SDS and CTAB. This fact suggests that most of the ion radicals exist in the bulk phase by the electric repulsion when the ion radicals have the same charge as the micellar surface. On the other hand, when the ion radicals have an opposite charge to that of the micellar surface, they are trapped on the surface and diffuse with the micelles. In any case, the parent molecules (BQ and AN) predominantly exist in the micelles. A diffusion model, which takes into account of the equilibrium between the micellar surface and bulk phase, can reproduce the observed micellar concentration dependence of  $D$  and the equilibrium constants of the transient radicals are determined.

## 1. Introduction

Because micelles prepare local hydrophobic environments in polar aqueous solution inhomogeneously, they can present a special reaction field. Chemical reactions in micelles can be very different from those in homogeneous solutions.<sup>1</sup> So far, many chemical reactions in various micellar systems have been investigated extensively.<sup>2–9</sup> The reaction dynamics are greatly influenced by the molecular dynamics in these systems. The following questions are important for elucidating the reactions in micellar systems: How do the solutes and chemically active (intermediate) molecules distribute in the micellar phase and the bulk phase? How does the distribution depend on the molecular size, shape, and polarity, or how are the diffusion processes affected by the presence of the micelles? For characterizing such properties, the micellar surface, the Stern layer, which has a few angstrom width, plays an important role, because in many cases the trapped solute molecules may exist in the micellar surface rather than in the micellar core.<sup>10</sup> The strong electric field ( $\sim 10^3$  V/m) is one of the remarkable properties of the micelles when one regards it as a reaction field. For example, the micellar electric field may manifest itself in the charge separation or electron transfer reaction. In homogeneous solutions, the created radicals are frequently quenched immediately by fast reverse electron transfer processes. However, on the micellar surface, one of the ion radical pair could be thrown out to the bulk phase by the electronic repulsion. Hence, the charge separation efficiency and the lifetimes of the ion radicals are expected to increase remarkably. Such an effect has been actually observed by using the transient absorption (TA) method<sup>3–6</sup> and the time-resolved EPR<sup>7–8</sup> in ionic micellar

solutions. For example, Wallace and co-workers reported biphotonic ionization processes of pyrene, triphenylene, and perylene in anionic micellar solution of sodium dodecyl sulfate (SDS) probed by the TA method.<sup>3</sup> They observed TA spectra of the hydrated electron and the cation radicals with high yields and concluded that the photoelectron is present in the bulk phase by the electric repulsion between the electron and the charge of the micellar surface.<sup>3</sup> Alkaitis et al. found that the monophotonic ionization yields of phenothiazine and  $N,N,N',N'$ -tetramethylbenzidine in SDS micelles are much higher than that in methanol by using the TA method.<sup>4</sup> The micellar effect to the electron transfer of pyrene to  $N,N$ -dimethylaniline (DMA) has been investigated by the time-resolved TA signals of the created ion radicals in the anionic micelle of SDS and in the cationic micelle of cetyl trimethylammonium bromide (CTAB).<sup>5</sup> The lifetime of the pyrene anion radical was found to be longer in CTAB than in SDS because the DMA cation radical was separated from the micellar phase to the bulk phase by the electric repulsion.<sup>5</sup> Similarly, efficient charge separations in ionic micellar solutions have been reported on Zinc porphyrin systems by TA,<sup>6</sup> EPR,<sup>7</sup> and fluorescence<sup>8</sup> measurements. An effect of the micellar charge was investigated for a benzophenone–aniline system probed by the line width of the CIDEP spectra of the created ion radicals.<sup>9</sup> Gao et al. measured the micellar solubilization equilibria of a stable anion of the carboxyproxyl radical to SDS anionic micelles by using the NMR paramagnetic relaxation method.<sup>11</sup> They reported that the ionic radical cannot enter the anionic micelles because of the electrostatic repulsion.<sup>11</sup>

However, despite these many reports on reactions in micellar solutions, there has been no direct quantitative measurement of the distribution between in the Stern layer and in the bulk phase of transient radicals, which shortly exist during the chemical reaction. Although Turro and co-workers measured exit rates of micellized radical pairs derived from the photocleavage of ketones by using the time-resolved ESR,<sup>12</sup> time-resolved flash

\* To whom correspondence should be addressed.

<sup>†</sup> Present address: Department of Electronic Science and Engineering, Kyoto University.

<sup>‡</sup> Kyoto University.

<sup>§</sup> Okayama University of Science.

CIDNP,<sup>13</sup> and laser flash spectroscopy,<sup>14</sup> not only exit rates but also rates of the entrance from the bulk phase to the micelles are required in order to obtain the distribution of the transient radicals in the micellar solution. The distribution between the bulk and micellar phases could be determined by a TA measurement, if the absorption spectrum or the absorbance of the transient species in the bulk phase is very different from those in the micellar phase. However, the difference is usually very small and such accurate measurement of the transient absorption spectrum to distinguish the difference in time domain is very difficult. To reveal the molecular dynamics or the distribution in the micellar solution, translational and rotational diffusion coefficients should be certainly direct and good quantities. In particular, although the translational coefficients ( $D$ ) of stable ions or neutral molecules in micellar solutions have been reported by using several methods,<sup>15</sup> direct measurement of these quantities as well as the distribution of any transient ion radical have never been reported in any micellar solution as far as we know.

Recently, we found that the transport properties of many transient radicals in organic solvents are different from those of stable molecules and interpreted the result in terms of enhanced intermolecular interactions to the matrix.<sup>16–19</sup> Hence, it is possible that the enhanced intermolecular interaction changes the distribution in the micelles from what we expect based on the data of the stable ionic or natural molecules. It is desirable to directly measure these quantities for transient reaction species during chemical reactions.

In this paper, we report  $D$  of a transient anion radical (benzoquinone anion radical) and a cation radical (aniline cation radical) created by the electron transfer reaction and also  $D$  of the neutral parent molecules simultaneously in anionic and cationic micellar solutions by using the transient grating (TG) method. The TG technique has been proven to be a very powerful method for the measurement of  $D$  of transient species.<sup>16–19</sup> Here, we focus our attention on the electric charge effect between the transient ionic radicals and the micelles.  $D$  of the parent molecules were also measured by using the Taylor dispersion (TD) method, which is a well-known technique to measure  $D$  of stable molecules precisely.

## 2. Experimental Section

The principle and the experimental set up for the TG technique have been described elsewhere in detail.<sup>16–21</sup> Briefly, the interference pattern of the excitation light intensity was created by crossing two laser pulses from an excimer laser ( $\sim 0.3$  mJ/cm<sup>2</sup>) [XeCl (308 nm); Lumonics Hyper-400]. Solute molecules in a sample cell (10 mm path length) were excited by this interference pattern. The excited molecules release the thermal energy by nonradiative relaxation, and the temperature of the sample is modulated (thermal grating). The excited molecules partly react, and the concentrations of the reactant and the products are also modulated (species grating). A probe beam from a He–Ne laser was partly diffracted (TG signal) by these gratings.<sup>20</sup> The TG signal was detected by a photomultiplier tube (Hamamatsu R-928) after isolation from random scattering light with a pinhole and a glass filter (Toshiba R-62), recorded with a digital oscilloscope (Tektronix 2430A), and analyzed with a microcomputer. The signals were averaged about 320 times to improve the S/N ratio. The fringe spacing was calculated from the decay of the thermal grating signal of benzene solution containing a trace of Methyl Red under the same experimental configuration.<sup>21</sup>

The experimental set up for the TD method have been reported.<sup>22–23</sup> Briefly, a sample solution was injected into a

solvent flowing through a capillary tube made of stainless steel. The length and diameter of the capillary tube were 50 m and 0.5 mm. This tube was coiled in a 0.30–0.35 m circle and placed in a temperature-controlled water bath. The concentration profile of the solution at the end of the stream was detected by a spectroscopic detector.  $D$  was calculated from the residence time and the width of the detected peak of solute concentration profile.

For the transient absorption (TA) measurement, the sample was excited by the excimer laser ( $\sim 5$  mJ/cm<sup>2</sup>) and probed by a 100W Xe lamp. The probe light was monochromated with a Spex model 1704 monochromator and detected by the photomultiplier.

Sodium dodecyl sulfate (SDS), cetyltrimethylammonium bromide (CTAB), and distillate water were purchased from Nacalai Tesque and used without further purification. The concentrations of SDS and CTAB were 0.01–0.1M, which were larger than the critical micellar concentration (cmc) of SDS (8.2mM) and CTAB (0.92mM). Benzoquinone (BQ) was purified by the recrystallization. Aniline (AN) was purified by the vacuum distillation. These solutes were purchased from Nacalai Tesque. Typical concentrations of the solutes were  $\sim 10^{-2}$  M. Sample solutions were deoxygenated by the nitrogen bubbling method and replaced by a fresh one after every  $\sim 1000$  shots of the excitation laser pulses. The sample solution was slowly stirred by a micromagnetic stirrer to dissipate the subsequence reaction product away from the excitation region. pH of micellar solutions were measured by a pH meter (Horiba) as 6.7 and 6.0 for SDS (0.1 M) and CTAB (0.1 M) solutions, respectively.

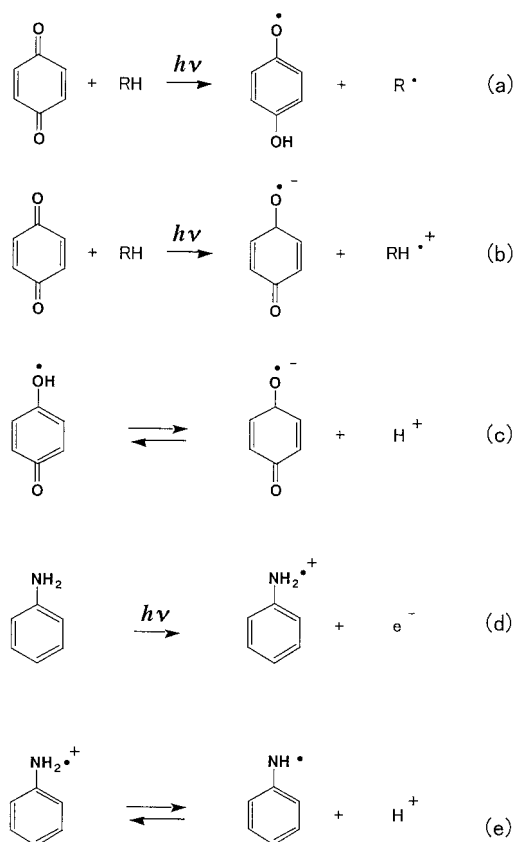
## 3. Results

**3.1 Photochemical Reactions in Micellar Solutions.** The photochemical reaction processes of benzoquinone (BQ)<sup>24–26</sup> and aniline (AN)<sup>27–28</sup> in water have been reported as Scheme 1. Benzosemiquinone radical (BQH $\cdot$ ) and anion radical (BQ $\cdot^-$ ) are created from the lowest excited triplet state of BQ by the hydrogen abstraction reaction (process a) and the electron transfer (process b) with the solvent (RH). The neutral radical (BQH $\cdot$ ) and the anion radical (BQ $\cdot^-$ ) are in equilibrium (process c). This equilibrium completes within 10  $\mu$ s after the creation of the radical.<sup>19</sup> Adams and Michel reported that  $pK_a$  of this equilibrium is 4.0.<sup>24</sup> Therefore, in an aqueous solution (pH = 7), BQ $\cdot^-$  is created dominantly. On the other hand, the cation radical of AN (AN $\cdot^+$ ) is directly created by the one-photon ionization in water (process d).<sup>27</sup> The created cation radical (AN $\cdot^+$ ) and the neutral radical (AN $\cdot$ ) are in equilibrium (process e). Land and Porter reported  $pK_a = 7.0$  for this equilibrium.<sup>28</sup> Therefore, in aqueous solution (pH = 7), both AN $\cdot^+$  and AN $\cdot$  are produced.

The photochemical reactions of BQ and AN in the SDS and CTAB solutions were studied by the transient absorption (TA) method. Figure 1a shows the observed TA spectra at a 100 ms time delay after the excitation of BQ in the SDS and CTAB solutions. A similar TA signal was observed for BQ in pure water. Reported spectra of BQ $\cdot^-$ <sup>25</sup> in water are also shown in Figure 1. The observed TA spectrum is similar to the reported one of BQ $\cdot^-$  in water. Therefore, we conclude that BQ $\cdot^-$  is created mainly from BQ not only in water but also in both the SDS and CTAB solutions. We believe that the counterion should be separated from BQ $\cdot^-$  quickly because the decay of BQ $\cdot^-$  is slow. On this time scale, it can be considered as the escaped (isolated) radical.

Figure 1b shows the observed TA spectra at a 100 ms time delay after the excitation of AN in the SDS and CTAB solutions

## SCHEME 1



together with reported spectra of AN $\cdot^+$  and AN $\cdot$  in water.<sup>27</sup> In this system, although the micellar charge may influence the pK<sub>a</sub>, we ascertained that both AN $\cdot^+$  and AN $\cdot$  are created in both SDS and CTAB solutions from the TA measurement. Decays of all these TA signals are well described by the second order kinetics and the half-lifetime of the TA signal is a few milliseconds. This fact suggests that the termination processes are mainly the radical recombination. As the excitation laser power for the TG measurement ( $\sim 0.3$  mJ/cm<sup>2</sup>) is weaker than that of the TA measurement ( $\sim 5$  mJ/cm<sup>2</sup>), the half-lifetime of the radicals for the TG measurement should be much longer than that for the TA measurement.

**3.2. D in Aqueous Solution.** Before examining the molecular diffusion in the micellar solutions, the TG signals in water were analyzed. The time profile of the TG signal after photoexcitation of BQ in water is shown in Figure 2. The square root of the TG signal ( $I_{TG}^{1/2}$  in the entire region) can be fitted by a sum of four exponential functions.

$$I_{TG}(t)^{1/2} = \left| \sum_{i=1}^4 a_i \exp(-k_i t) \right| \quad (1)$$

where,  $k_1 \gg k_2 > k_3 > k_4$  are the decay constants and  $a_1$  through  $a_4$  are the preexponential factors. For reproducing the observed signal, we found that the sign of  $a_i$  should be  $a_1 < 0$ ,  $a_2 > 0$ ,  $a_3 < 0$ , and  $a_4 > 0$ . The origin of each component is assigned as follows.

In the previous papers, we described that the time profile of the TG signal is given by the following equation.<sup>17–19</sup>

$$I_{TG}(t)^{1/2} = |\delta n_{th}^o \exp(-D_{th} q^2 t) - \sum_P \delta n_P^o \exp(-D_P q^2 t) + \sum_R \delta n_R^o \exp(-D_R q^2 t - 1/\tau_R)| \quad (2)$$

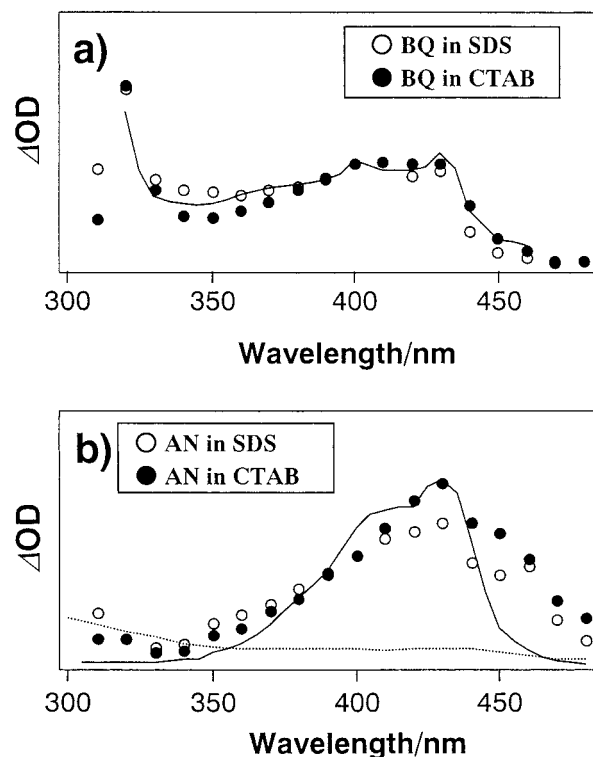


**Figure 1.** (a) Transient absorption spectra at a 100ms delay after the excitation of BQ in the SDS aqueous solution (○) and BQ in the CTAB aqueous solution (●). Solid line is the reported spectrum of BQ $\cdot^-$  in water (ref 29). (b) Transient absorption spectra at a 100 ms delay after the excitation of AN in the SDS aqueous solution (○) and AN in the CTAB aqueous solution (●). Solid line and broken line are the reported spectrum of AN $\cdot^+$  and neutral radical in water (ref 27).

where  $q$  is the grating wavenumber [ $q = 2\pi/\Lambda$  ( $\Lambda$ ; fringe length)]. The first term of eq 2 represents the thermal grating and  $\delta n_{th}^o$  is the initial refractive index change just after the excitation.  $\delta n_P^o$  and  $\delta n_R^o$  are the initial refractive index changes by the species grating of the parent molecules and the radicals, respectively. The refractive index change of the thermal grating is negative ( $\delta n_{th}^o < 0$ ) and the refractive index change of the species grating of this systems should be positive ( $\delta n_P^o, \delta n_R^o > 0$ ).  $D_{th}$  is the thermal diffusivity of the solvent, and  $D_P$  and  $D_R$  are the diffusion constants of the parent molecules and the radicals, respectively.  $\tau_R$  is the lifetime of the radicals when the termination of the radical follows the first-order kinetics. Since  $D_{th}$  is much larger than  $D_P$  or  $D_R$ , it is apparent that the  $a_1 \exp(-k_1 t)$  term in eq 1 represents the thermal grating term. Using the TA method, Ononye and Bolton found that photoexcited BQ abstracts a hydrogen atom from water and BQ $\cdot^-$  is created immediately by the proton dissociation.<sup>24</sup> Therefore, BQ and BQ $\cdot^-$  shall be observed in the TG signal. In the same way to our previous reports in homogeneous solvents,<sup>16–17,19</sup> we can assign each term based on the sign of  $a_i$ . Finding  $a_3 < 0$  and  $a_4 > 0$ , we can assign  $a_3 \exp(-k_3 t)$  and  $a_4 \exp(-k_4 t)$  terms to the species gratings of the parent molecule (BQ) and the radical (BQ $\cdot^-$ ), respectively. From the sign of the preexponential factor, the component 2 should be attributed to a molecule that is produced by the reaction. However, since the decay rate constant,  $k_2$ , is much larger than we expect for a typical  $D$  of an organic molecule of this size in water, it cannot be the species gratings of BQ or BQ $\cdot^-$ . The origin of the component 2 is unknown at present. If the sample was not deoxygenated well, the relative intensity of  $a_2$  becomes larger while those of  $a_3$  and  $a_4$  become smaller. Probably, component 2 may be due to

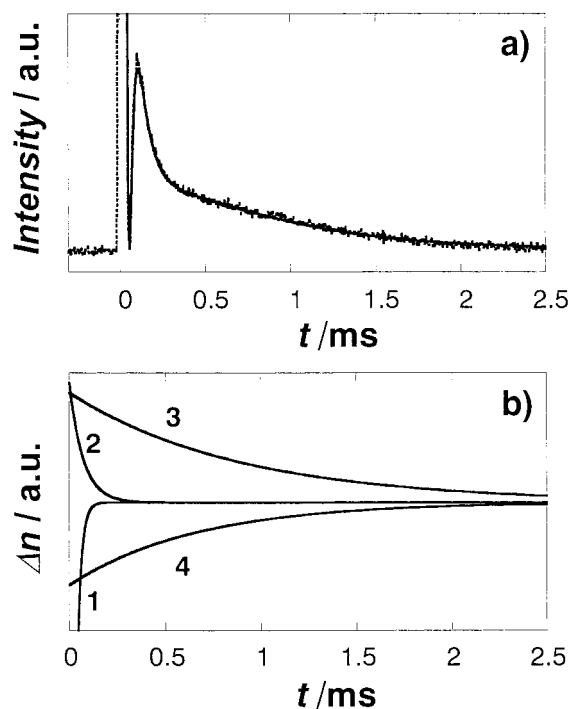


**Figure 2.** (a) Time profile of the TG signal after the photoexcitation of BQ in water at 23 °C (dotted line) and the best fitted curve (solid line) by eq 1. (b) Four components for the fitting in (a) are shown separately. The assignments of these components are 1; thermal grating, 3 and 4; species grating of BQ and that of BQ<sup>•−</sup>, respectively. Component 2 comes from unknown species.

**TABLE 1: Diffusion Constants of Parent Molecules in Water, SDS (0.1 M), and CTAB (0.1 M) Probed by the Taylor Dispersion Method**

solute	solvents	$D/10^{-9} \text{ m}^2 \text{ s}^{-1}$
benzoquinone	water	$1.02 \pm 0.03$
	SDS	$0.73 \pm 0.03$
	CTAB	$0.82 \pm 0.02$
aniline	water	$0.85 \pm 0.04$
	SDS	$0.202 \pm 0.0003$
	CTAB	$0.387 \pm 0.001$

a molecule created by a reaction between the radical and oxygen dissolved in the solution.

On the basis of these assignments,  $k_1$ ,  $k_3$ , and  $k_4$  are given by

$$k_1 = D_{\text{th}} q^2 \quad (3a)$$

$$k_3 = D_{\text{P}} q^2 \quad (3b)$$

$$k_4 = D_{\text{R}} q^2 + 1/\tau_{\text{R}} \quad (3c)$$

Since  $k_1$  is much larger than  $k_3$  and  $k_4$ ,  $k_1$  can be determined accurately by the least-squares fitting. On the other hand, because  $k_3$  and  $k_4$  are rather close, we cannot avoid a larger ambiguity for  $k_3$  and  $k_4$ . Therefore, we tried to reduce the number of adjustable parameters for the fitting by measuring  $D$  of BQ.

We used the TD method for determining  $D$  of BQ. The results are shown in Table 1.  $D_{\text{P}}$  of BQ in water was obtained as  $1.02 \times 10^{-9} \text{ m}^2 \text{ s}^{-1}$  from TD. By using this  $D_{\text{P}}$ , we fit the time profile of the TG signal (in Figure 2a) by the nonlinear least-squares method with eq 1. The solid line in Figure 2a is the best fitted line, and the time profiles of the four components are shown separately in Figure 2b.

The time profile of the TA signal indicates that the subsequent reaction is the second-order reaction. If the decay of the TG

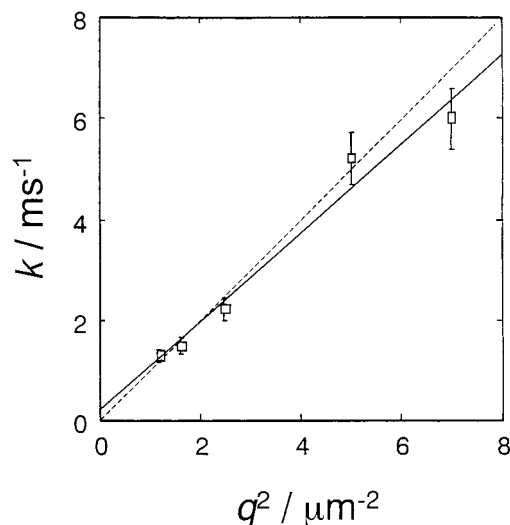


**Figure 3.** Relationship between the decay rate constants ( $k$ ) of the TG signal of BQ<sup>•−</sup> and  $q^2$  in water. The solid line is best-fitted line by the least-squares method. The dotted line is calculated  $k$  for BQ from  $D$  measured by the TD method.

**TABLE 2: Diffusion Constants ( $D$ ) of Benzoquinone Anion Radicals and Aniline Action Radicals in Water, SDS (0.1 M), and CTAB (0.1 M) Probed by the Transient Grating Method**

solute	solvents	$D/10^{-9} \text{ m}^2 \text{ s}^{-1}$
benzoquinone anion radicals	water	$0.9 \pm 0.2$
	SDS	$0.94 \pm 0.05$
	CTAB	$0.55 \pm 0.04$
aniline cation radicals	water	—
	SDS	$0.08 \pm 0.01$
	CTAB	$0.76 \pm 0.03$

signal due to the diffusion process is much faster than that of the subsequent reaction,  $\tau_{\text{R}}$  in eq 3c could be approximately replaced by the half-lifetime of the concentration of the ion radical.<sup>16</sup> On the other hand, if the decay due to the subsequent reaction is much faster than that of the diffusion process, eq 3c is no longer satisfied and  $k$  vs  $q^2$  plot should not be linear.<sup>18</sup> The relationship between  $k$  and  $q^2$  is shown in Figure 3. The small intercepts with the ordinate and good linearity of these plots indicate that the diffusion process should be faster than the subsequent reaction and eq 3c should be satisfied. This fact is consistent with the long lifetimes of the radicals observed by the TA measurement. Therefore,  $D$  can be determined from the slopes of the  $q^2$  plot (Figure 3). The obtained  $D$  are listed in Table 2.  $D$  of BQ and BQ<sup>•−</sup> are very similar each other ( $D_{\text{P}}/D_{\text{R}} \sim 1.1$ ). This similarity between  $D_{\text{P}}$  and  $D_{\text{R}}$  in water is very different from what we obtained in organic solutions (e.g.  $D_{\text{P}}/D_{\text{R}} \sim 2.8$  in ethanol and 2.7 in 2-propanol<sup>16</sup>) but consistent with the radical diffusion behavior in water.<sup>19</sup> We could not obtain  $D$  of AN and AN<sup>•+</sup> in water because the TG signal was too weak to be analyzed.

**3.3.  $D$  in Micellar Solution.** The time profile of the TG signal of BQ in the SDS (0.1M) solution is shown in Figure 4. It should be noted that the time range of this signal is much longer than that in Figure 2. This TG signal can be also fitted by eq 1 ( $i = 4$ ). The fitted line and the time profiles of the decomposed four components are shown in Figure 4, parts a and b. Obviously, the fastest component ( $a_1$ ) should be attributed to the thermal grating and the decays of the negative ( $a_2$ ) and positive ( $a_3$ ) contributions of slow components are attributed to the parent molecules and the radicals, respectively. The fast decay component observed in water (component 2 in Figure 2) did not appear in this system. On the other hand, another slow decay



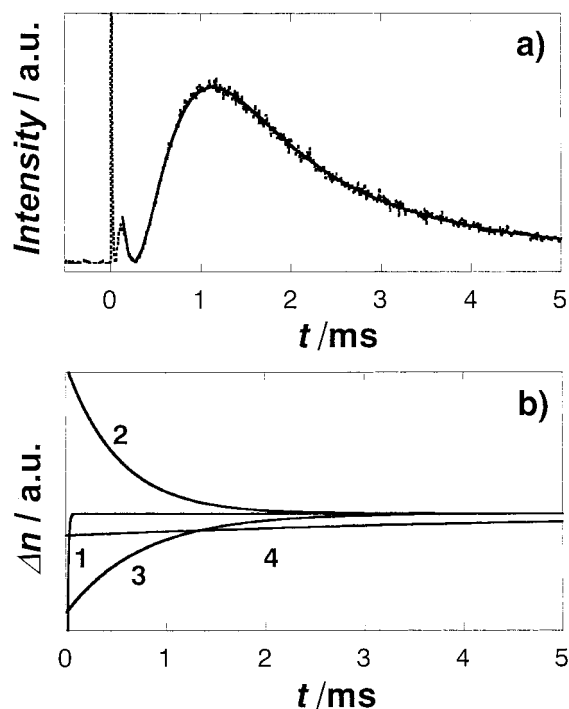


**Figure 4.** (a) Time profile of the TG signal after the photoexcitation of BQ in the SDS solution at 23 °C (dotted line) and the best fitted curve (solid line) by eq 1. (b) Fore components for the fitting in (a) are shown separately. The assignments of these components are 1; thermal grating, 2 and 3; species grating of  $\text{BQ}^{\bullet-}$  and that of BQ, respectively. Component 4 comes from unknown species.

component ( $a_4$ ) appeared. The origin of this component is unknown at present. It could be due to an impurity molecule that located in the micellar phase because the decay rate constant of the slowest component ( $k_4$ ) is much smaller than those of the other ones. (One of possible candidates of the impurity is hydroquinone that is created by reduction of BQ in water. Hydroquinone forms aggregates, which are probably located in the micellar phase.)

Again, it is difficult to determine the accurate  $D$  values by the curve fitting in this case, because the S/N ratio of this signal was much smaller than that of Figure 2. Therefore, we reduced the number of adjustable parameters as follows. First, we should note that the ratio of the TG signal intensities between the radicals and the parent molecules ( $a_2/a_3=1.3$ ) is determined by that of the refraction index changes between the radicals and the parent molecules at the wavelength of the probe beam (633 nm). This ratio in micellar solutions should be similar to that in water because the TA spectra are not so much different in water and in micellar solutions. Hence, the ratio determined in water was used for the fitting in the micellar solution case. Second, the decay rate constant ( $k_2$ ) was fixed to the calculated values from  $D_p$  (Table 1) and  $q^2$ . Using these reduction methods, we can fit the TG signal unambiguously. The time profile of the TG signal of BQ in the CTAB (0.1 M) solution is shown in Figure 5.

The plots of the rate constants of BQ and  $\text{BQ}^{\bullet-}$  against  $q^2$  in the SDS and CTAB solutions are shown in Figure 6. They show a good linear relationship. We determined  $D_R$  in the SDS and CTAB solution from the slopes of this plot and listed in Table 2.

Figure 7 shows the TG signals of (a) AN in the SDS (0.1 M) solution and (b) AN in the CTAB (0.1 M) solution. Since the absorption band of  $\text{AN}^{\bullet+}$  is stronger and closer to the probe wavelength (633 nm) than that of  $\text{AN}^{\bullet}$  (Figure 1), the species

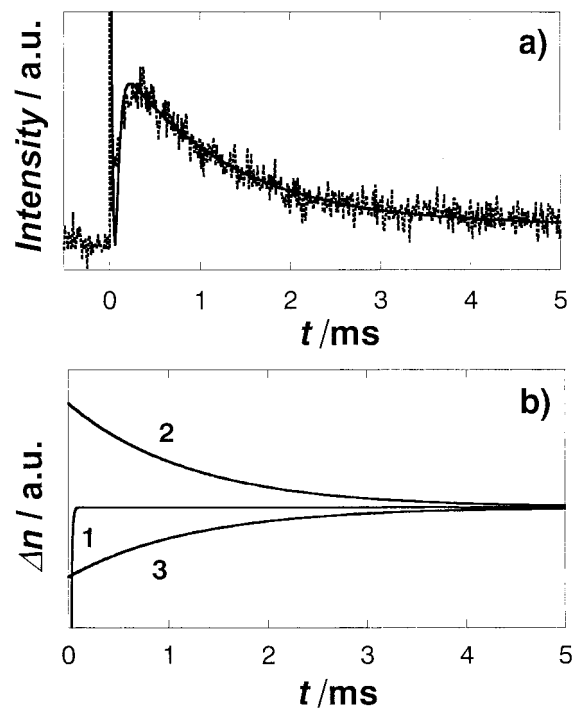


**Figure 5.** (a) Time profile of the TG signal after the photoexcitation of BQ in the CTAB solution at 23 °C (dotted line) and the best fitted curve (solid line) by eq 1. (b) Three components in the grating signal are shown separately (text). The assignments of these components are 1; thermal grating, 2 and 3; species grating of BQ and that of  $\text{BQ}^{\bullet-}$ , respectively.

which mainly contributes to the TG signal should be  $\text{AN}^{\bullet+}$ . The TG signal of AN in the SDS solution is quite similar to that of BQ in the CTAB solution, while the TG signal of AN in the CTAB solution is quite similar to that of BQ in the SDS solution. Those signals in the SDS and CTAB solution can be also fitted in a way similar to the case of BQ, and the decay rates of the TG signal due to  $\text{AN}^{\bullet+}$  are determined. The  $k$  vs  $q^2$  plots of  $\text{AN}^{\bullet+}$  are shown in Figure 8, and obtained  $D$  are listed in Table 2.

$D$  of  $\text{BQ}^{\bullet-}$  in the SDS solution and  $\text{AN}^{\bullet+}$  in the CTAB solution are similar to  $D$  of  $\text{BQ}^{\bullet-}$  in the aqueous solution, while  $D$  of  $\text{BQ}^{\bullet-}$  in the CTAB solution,  $\text{AN}^{\bullet+}$  in the SDS solution, and the parent molecules in both micellar solutions are smaller than  $D$  in water. This fact suggests that the diffusion process of the ion radicals in ionic micellar solutions is very sensitive to the electric charge of the ion radicals and micelles.

## 4. Discussion

**4.1. Interaction between the Ion Radicals and the Micellar Surface.** Our results show that, when the charge of ion radicals and micellar surface are of the same sign ( $\text{BQ}^{\bullet-}/\text{SDS}$ ,  $\text{AN}^{\bullet+}/\text{CTAB}$ ),  $D$  of the ion radicals are larger than those of the parent molecules and close to  $D$  in aqueous solutions. The large  $D$  imply that most part of the ion radicals exist in the bulk phase. Probably, the created ion radicals are thrown out to the bulk phase by the electric repulsion even though the parent molecules stay in the micelles and the photochemical reaction takes place inside the micelles. (As described in section 3.1, the effect of the counterion can be neglected on the time scale of the diffusion measurement.) On the other hand, when the charge of the ion radicals and the micellar surface are opposite ( $\text{BQ}^{\bullet-}/\text{CTAB}$ ,  $\text{AN}^{\bullet+}/\text{SDS}$ ),  $D$  of the ion radicals are smaller than  $D$  of the parent molecules and rather close to  $D$  of the micelles. The self-diffusion constants of the micelles are reported as  $0.07 \times 10^{-9}$

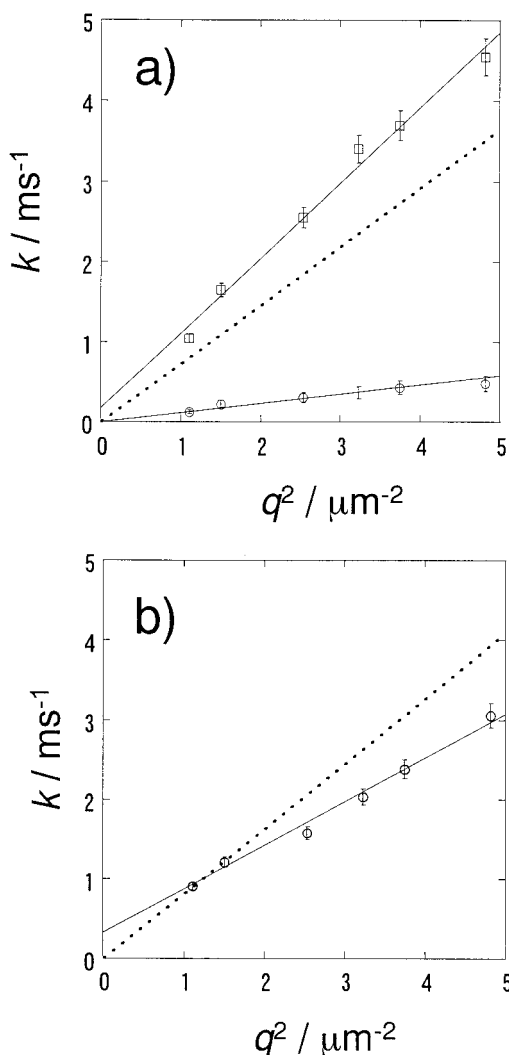


**Figure 6.** Relationship between the decay rate constants of the TG signal ( $k$ ) of  $\text{BQ}^{\bullet-}$  ( $\square$ ) and  $q^2$  (a) in the SDS and (b) in the CTAB solution ( $\circ$ ). The solid line is the best-fitted line by the least-squares method. The dotted line is calculated  $k$  for BQ from  $D$  measured by the TD method. Unknown component is also plotted ( $\circ$ ) in (a).

$\text{m}^2 \text{s}^{-1}$  and  $0.04 \times 10^{-9} \text{m}^2 \text{s}^{-1}$  for 0.1 M SDS<sup>29</sup> and CTAB,<sup>30</sup> respectively. (The radii of micells of SDS and CTAB were calculated from these self-diffusion coefficients as 2.22 nm and 3.09 nm, respectively.) This fact suggests that a part of the ion radicals and the parent molecules exist in the micellar phase (on the micellar surface). The equilibrium constant of the distribution will be described later. The dominant presence of BQ and AN in micelles may be due to the hydrophobic nature. It was reported that aromatic hydrocarbons such as benzene and toluene stay in the micellar core by the strong hydrophobic character, but the hydrophobic solute which have a hydrophilic group ( $-\text{OH}$ ,  $=\text{O}$ , or  $-\text{NH}_2$ ) are trapped on the micellar surface (Stern layer) rather than in the micellar core.<sup>10</sup> Considering these facts, we think that BQ and AN are located on the Stern layer rather than in the micellar core. This location might be one of the causes of the efficient releasing and trapping of the photochemically created ion radicals.

Because of the electric charge of the ion radicals, we could expect that the ion radicals are located in water rather than in the nonpolar micelles. However,  $D$  measured in this study strongly suggests that the created ion radicals are trapped on the micellar surface by the Coulomb force between the charges of ion radicals and the Stern layer.

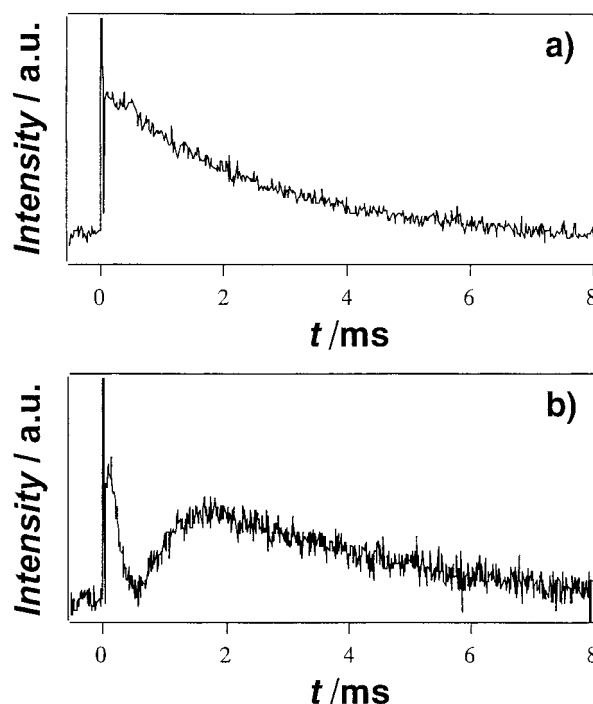


**Figure 7.** Time profile of the TG signal after the photoexcitation of (a) AN in the SDS solution and (b) that of AN in the CTAB solution at 23 °C.

So far, many groups studied the electric interaction between ionic radicals and micelles indirectly.<sup>2–9</sup> For example, Kautusins-Razem et al.<sup>5</sup> measured the lifetimes of the ion radicals created by the electron transfer between pyrene and *N,N*-dimethylaniline (DMA) in methanol (6  $\mu\text{s}$ ), CTAB cationic micelle (500  $\mu\text{s}$ ), SDS anionic micelle (66.6  $\mu\text{s}$ ), and Igepal neutral micelle (13.1  $\mu\text{s}$ ). They interpreted the long lifetime in the CTAB micellar solution by the hindrance of the reverse electron transfer due to the electronic repulsion between the cation radical of dimethylaniline and cationic micellar surface of CTAB. (As pyrene is a large molecule, it hardly exists in water regardless of the micellar charge.) As another example, the line width of the EPR spectra of the benzophenone (BP) anion radical was found to be sharp in the SDS micellar solution, while it was broad in the CTAB micellar solution.<sup>9</sup> The different line width was interpreted in terms of the different environment of the radical; that is, the anion radical trapped on the cationic micelle (CTAB) gives the broader spectrum by the motional restriction. In this study, we obtain more direct evidence for the trapping of the ion radicals from the  $D$  measurements. One of advantages of this method is that it enables us to measure the equilibrium constant of the distribution of the transient radicals between bulk water and the micelles as we will show in the next section.

**4.2. Micellar Concentration Dependence of  $D$ .** To study the dynamics of the ion radicals in more detail, the micellar concentration dependence of  $D$  was measured.  $D$  at various micellar concentrations for BQ and  $\text{BQ}^{\bullet-}$  are listed in Table 3 and plotted in Figure 9. Micellar concentrations  $[M]$  are estimated by the following equation.

$$[M] = \frac{[\text{Det}] - \text{cmc}}{\bar{n}} \quad (4)$$

where,  $[\text{Det}]$  is the concentration of detergent (SDS or CTAB) and  $\bar{n}$  is the mean micelle aggregation number, which is  $\sim 60$  (SDS)<sup>31</sup> and  $\sim 90$  (CTAB).<sup>32</sup> The critical micellar concentration (cmc) of SDS and CTAB are 8.2 mM and 0.92 mM, respec-

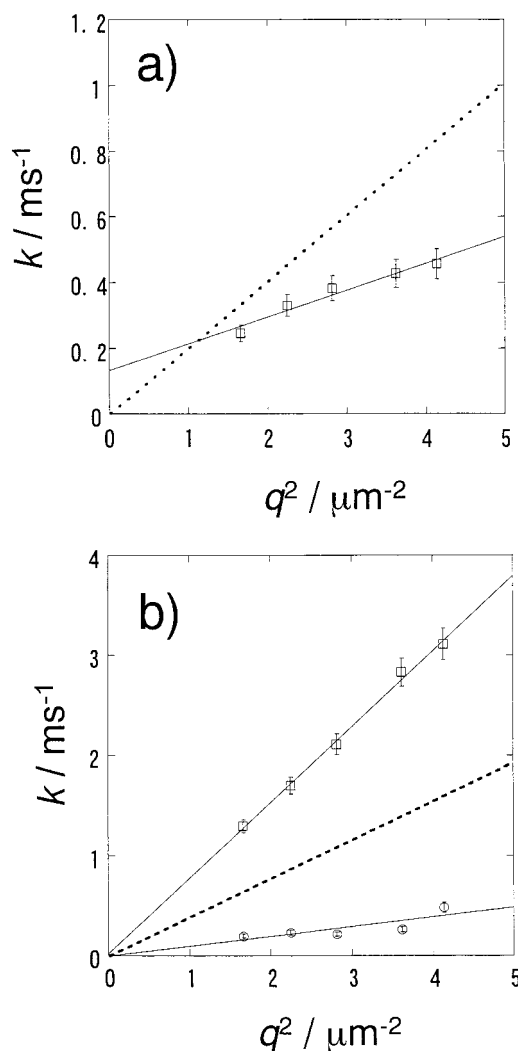


**Figure 8.** Relationship between the decay rate constants of the TG signal ( $k$ ) of  $\text{AN}^{*+}$  ( $\square$ ) and  $q^2$  (a) in the SDS and (b) in the CTAB solution. The solid line is the best-fitted line by the least-squares method. The dotted line is calculated  $k$  for AN from  $D$  measured by the TD method. Unknown component is also plotted ( $\circ$ ).

**TABLE 3: Micellar Concentration Dependence of the Diffusion Constants ( $D$ ) of Benzoquinone Anion Radical in SDS and CTAB**

[SDS] or [CTAB]/M	$D/10^{-9} \text{ m}^2 \text{ s}^{-1}$	
	in SDS	in CTAB
0.01	1.0	0.81
0.02	0.97	0.79
0.04	0.99	0.62
0.06	0.94	0.59
0.08	0.91	0.57
0.10	0.94	0.55

tively.<sup>33</sup>  $D$  of  $\text{BQ}^{\bullet-}$  in the SDS solution does not depend on the micellar concentration and always close to  $D$  in the aqueous solution (broken line in Figure 9). This fact implies that most of  $\text{BQ}^{\bullet-}$  exists in the bulk phase in the SDS solution at any concentration of the micelle.

On the other hand,  $D$  of  $\text{BQ}^{\bullet-}$  in the CTAB solution depends on the micellar concentration.  $D$  of  $\text{BQ}^{\bullet-}$  become smaller with increasing the micellar concentration and closer to  $D$  of the micelle. It suggests that the relative amount of the solute molecules in the micellar phase compared with that in the bulk phase increases with increasing the micellar concentration. In the following, we quantitatively explain the observed micellar

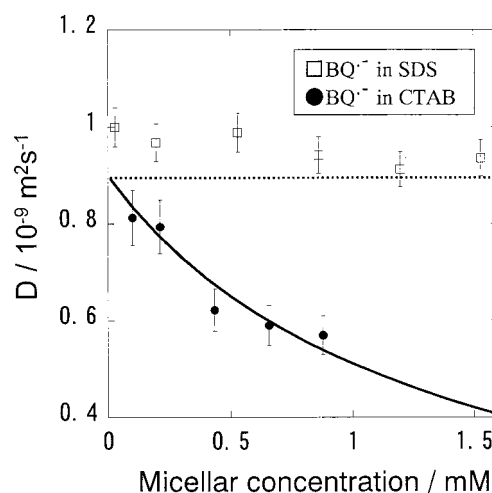
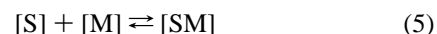


**Figure 9.** Micellar concentration dependence of  $D$  of  $\text{BQ}^{\bullet-}$  in SDS solution ( $\square$ ) and CTAB ( $\bullet$ ). The dotted line is  $D$  of  $\text{BQ}^{\bullet-}$  in water. The curved lines are calculated  $D$  by eq 9 with  $K_s = 840 \pm [\text{M}^{-1}]$ .

concentration dependence of  $D$  by taking into account the equilibrium between the bulk phase and the micelles.

The solubility of a solute molecule in the micellar solution may be expressed by the equilibrium between the micellar phase and the bulk phase as<sup>34</sup>



where  $[\text{S}]$  and  $[\text{SM}]$  are the concentrations of the solute in the bulk phase and in the micellar phase, respectively.  $[\text{M}]$  is the concentration of the micelles obtained by eq 4.

Generally, the equilibrium constant ( $K_s$ ) is given by

$$K_s = \frac{[\text{SM}]}{[\text{S}][\text{M}]} \quad (6)$$

Usually,  $K_s$  has been measured from the data of solubilities to water and micellar solution<sup>35</sup> or micellar concentration dependence of the absorbance of the solute.<sup>36</sup> However, the value may not be accurate if the absorption spectra in water and micelles are similar. In particular, it could be very difficult to measure a time-dependent TA spectrum of a transient species accurately enough. Measurement of solubility for transient species should be extremely difficult. Here we determined  $K_s$  from  $D$  as follows.

As exist rate constants of solute molecules from micelles to bulk phase are usually about  $10^6 \text{ s}^{-1}$  order,<sup>5,11–13</sup> equilibrium (5) should be completed within a few  $\mu\text{s}$ . After the equilibrium is achieved,  $D$  of the solute ( $D_s$ ) can be described by the average between  $D$  in the bulk phase ( $D_b$ ) and in the micellar phase ( $D_m$ ).<sup>37</sup>

$$D_s = \frac{D_m[\text{MS}] + D_b[\text{S}]}{[\text{MS}] + [\text{S}]} \quad (8)$$

From eqs 8 and 6, we obtained the following relationship.

$$D_s = D_m \left[ 1 + \frac{1}{1 + K_s[\text{M}]} \left( \frac{D_b}{D_m} - 1 \right) \right] \quad (9)$$

By using eq 9 with  $D_m$  measured by the TD method,  $K_s$  of BQ were obtained as  $292 [\text{M}^{-1}]$  (in SDS) and  $196 [\text{M}^{-1}]$  (in CTAB).

The micellar concentration dependence of  $D$  of  $\text{BQ}^{\bullet-}$  in CTAB can be fitted by eq 9 and the fitted line is shown in Figure 9. For the best fitting,  $K_s = 840 \pm 79 \text{ [M}^{-1}\text{]}$  was obtained for  $\text{BQ}^{\bullet-}$ . On the other hand, in the case of  $D$  of  $\text{BQ}^{\bullet-}$  in SDS,  $K_s$  is nearly 0  $[\text{M}^{-1}]$ . Generally, measurement of the molecular distribution between micelle and bulk phase is not easy, in particular for transient species as mentioned above. Hence there is no data on this quantity of any transient species, although this information is important to analyze chemical reaction in micellar solution. Using the TG method, we can measure this quantity even for the transient species for the first time.

## 5. Conclusion

Diffusion constants ( $D$ ) of the photochemical intermediate anion radicals of BQ ( $\text{BQ}^{\bullet-}$ ) and the cation radical of AN ( $\text{AN}^{\bullet+}$ ) in the anionic micellar solution of SDS and the cationic micellar solution of CTAB were measured by using the transient grating (TG) method. It is found that  $D$  of  $\text{BQ}^{\bullet-}$  in the SDS solution and  $\text{AN}^{\bullet+}$  in the CTAB solution are larger than those of the parent molecules, while in BQ/CTAB and AN/SDS cases,  $D$  of both the ion radicals and the parent molecules are similar. These observations are consistently explained in term of the Coulomb interaction between the ion radicals and the charge in the Stern layer of the micelles. The micellar concentration dependence of  $D$  is also investigated by BQ in the SDS and the CTAB solutions.  $D$  of  $\text{BQ}^{\bullet-}$  in the SDS solution are insensitive to the micellar concentration and similar to  $D$  of  $\text{BQ}^{\bullet-}$  in neat water. However,  $D$  of BQ in the SDS solution and  $D$  of BQ and  $\text{BQ}^{\bullet-}$  in the CTAB solution are sensitive to the concentration of the micelle. The observed micellar concentration dependence of  $D$  can be reproduced by using a diffusion model, which takes into account the equilibrium between the micellar surface and bulk phase. Using this method, we could determine the equilibrium constants of the transient radicals in micellar solutions for the first time.

**Acknowledgment.** The authors would like to thank Prof. Y. Tanimoto (Hiroshima University) for valuable suggestions and discussions. A part of this study was supported by Scientific Research Grant-In-Aids from the Ministry of Education, Science and Culture (No.08554021), Japan Society for the Promotion of Science, and Venture Business Laboratory in Kyoto University (KU-VBL).

## References and Notes

- (1) (a) Gebicki, J. M.; Hicks, M. *Nature* **1973**, *243*, 232. (b) Gebicki, J. M.; Hicks, M. *Chem. Phys. Liquid* **1976**, *16*, 142. (c) Hicks, M.; Gebicki, J. M. *Chem. Phys. Liquid* **1976**, *16*, 142. (d) Fromhertz, P. *Chem. Phys. Lett.* **1980**, *77*, 460. (e) Menger, F. M.; Jerkunica, J. M.; Johnston, J. C. *J. Am. Chem. Soc.* **1978**, *100*, 4676. (f) Menger, F. M.; Boyer, B. J. *J. Am. Chem. Soc.* **1980**, *102*, 5936.
- (2) (a) Menger, F. M. *Accounts Chem. Res.* **1979**, *12*, 111. (b) Menger, F. M.; Portnoy, C. E. *J. Am. Chem. Soc.* **1967**, *90*, 4404. (c) Lindquist, R. N.; Cordes, E. H. *J. Am. Chem. Soc.* **1968**, *90*, 1269.
- (3) Wallace, S. C.; Gratzel, M.; Thomas, J. K. *Chem. Phys. Lett.* **1973**, *23*, 359.
- (4) (a) Alkaitis, S. A.; Beck, G.; Gratzel, M. *J. Am. Chem. Soc.* **1975**, *97*, 5723. (b) Alkaitis, S. A.; Gratzel, M. *J. Am. Chem. Soc.* **1976**, *98*, 3549.
- (5) Katusin-Razem, B.; Wong, M.; Thomas, J. K. *J. Am. Chem. Soc.* **1978**, *100*, 1679.
- (6) (a) Brugger, P.-A.; Infelta, P. P.; Braun, A. M.; Gratzel, M. *J. Am. Chem. Soc.* **1981**, *103*, 320. (b) Darwent, J. R. *J. Chem. Soc., Chem. Commun.* **1980**, 805.
- (7) (a) Levstein, P. R.; van Willigen, H. *Chem. Phys. Lett.* **1991**, *184*, 415. (b) Hanaishi, R.; Ohba, Y.; Yamauchi, S.; Iwaizumi, M. *Bull. Chem. Soc. Jpn.* **1996**, *69*, 1533.
- (8) Costa, S. M. B.; Brookfield, R. L. *J. Chem. Soc., Faraday Trans. 2* **1986**, *82*, 991.
- (9) Hirata, T.; Miyagawa, K.; I'Haya, Y.; Murai, H. *Nippon Kagaku Kaishi* **1992**, *12*, 1423.
- (10) Hirose C.; Sepulveda, L. *J. Phys. Chem.* **1981**, *85*, 3689.
- (11) Gao, Z.; Wasylshen, R. E.; Kwak, J. C. T. *J. Chem. Soc., Faraday Trans.* **1991**, *87*, 947.
- (12) Wu, C.-H.; Jenks W. S.; Koptyug, I. V.; Ghatlia, N. D.; Lipson, M.; Tarasov, V. F.; Turro, N. J. *J. Am. Chem. Soc.* **1993**, *115*, 9595.
- (13) Turro, N. J.; Zimmt, M. B.; Gould, I. R. *J. Am. Chem. Soc.* **1983**, *105*, 6347.
- (14) Turro, N. J.; Wu, C.-H. *J. Am. Chem. Soc.* **1995**, *117*, 11031.
- (15) (a) Burkey, T. J.; Griller, D.; Lindsay, D. A.; Scaiano, J. C. *J. Am. Chem. Soc.* **1984**, *106*, 1983. (b) Chatenay, D.; Urbach, W.; Messenger, R.; Langevin, D. *J. Chem. Phys.* **1987**, *86*, 2343. (c) Kamenka, N.; Lindman, B.; Brun, B. *Colloid Polym. Sci.* **1974**, *252*, 144. (d) Stilbs, P. *J. Colloid Interface Sci.* **1982**, *87*, 385.
- (16) (a) Terazima, M.; Okamoto, K.; Hirota, N. *J. Phys. Chem.* **1993**, *97*, 13387. (b) Terazima, M.; Okamoto, K.; Hirota, N. *Laser Chem.* **1994**, *13*, 169. (c) Terazima, M.; Okamoto, K.; Hirota, N. *J. Chem. Phys.* **1995**, *102*, 2506. (d) Okamoto, K.; Terazima, M.; Hirota, N. *J. Chem. Phys.* **1995**, *103*, 10445. (e) Okamoto, K.; Hirota, N.; Terazima, M. *J. Phys. Chem. A* **1997**, *101*, 5380.
- (17) Okamoto, K.; Hirota, N.; Terazima, M. *J. Chem. Soc., Faraday Trans.* **1998**, *94*, 185.
- (18) Okamoto, K.; Hirota, N.; Terazima, M. *J. Phys. Chem. A* **1997**, *101*, 5269.
- (19) Okamoto, K.; Hirota, N.; Terazima, M. *J. Phys. Chem. A* **1998**, *102*, 3447.
- (20) Eichler, H. J.; Gunter, P.; Pohl, D. W. *Laser-Induced Dynamic Grating* (Springer, Berlin, 1986).
- (21) Terazima, M.; Okamoto, K.; Hirota, N. *J. Phys. Chem.* **1993**, *97*, 5188.
- (22) (a) Tominaga, T.; Yamamoto S.; Takanaka J. *J. Chem. Soc., Faraday Trans. 1*, **1984**, *80*, 91. (b) Tominaga, T.; Matsumoto, S.; Ishii, T. *J. Phys. Chem.* **1986**, *90*, 139. (c) Tominaga, T.; Matsumoto, S. *Bull. Chem. Soc. Jpn.* **1990**, *63*, 533.
- (23) Tominaga, T.; Tenma, S.; Watanabe, H. *J. Chem. Soc., Faraday Trans.* **1996**, *92*, 1863.
- (24) (a) Ononye, A. I.; Bolton, J. R. *J. Phys. Chem.* **1986**, *90*, 6270. (b) Adams, G. E.; Michel, B. D. *Trans. Faraday Soc.* **1967**, *63*, 1171.
- (25) Kimura, K.; Yoshinaga, K.; Tsubomura, H. *J. Phys. Chem.* **1967**, *71*, 4485.
- (26) Scheerer, R.; Gratzel, M. *J. Am. Chem. Soc.* **1977**, *99*, 865.
- (27) (a) Saito, F.; Tobita, S.; Shizuka, H. *J. Chem. Soc., Faraday Trans.* **1996**, *92*, 4177. (b) Yoshihara, T.; Yamaji, M.; Shizuka, H. *Chem. Phys. Lett.* **1996**, *261*, 431.
- (28) Land, E. J.; Porter, G. *Trans. Faraday. Soc.* **1963**, *59*, 2027.
- (29) Clifford, J.; Pethica, B. A. *J. Phys. Chem.* **1966**, *70*, 3345.
- (30) (a) Tominaga, T.; Nishinaka, M. *J. Chem. Soc., Faraday Trans.* **1993**, *89*, 3459. (b) Lindman, B.; Puyal, M.-C.; Kamenka, N.; Rymden, R.; Stilbs, P. *J. Phys. Chem.* **1984**, *88*, 5048.
- (31) (a) Rassing, J. E.; Sams, P. J.; Wyn-jones, E. *J. Chem. Soc., Faraday Trans. 2* **1974**, *70*, 1247. (b) Yekta, A.; Aikawa, M.; Turro, N. *J. Chem. Phys. Lett.* **1979**, *63*, 543. (c) Ikeda, S. *Colloid Polym. Sci.* **1991**, *269*, 49.
- (32) (a) Ikeda, S. *Colloid Polym. Sci.* **1991**, *269*, 49. (b) Imae, T.; Kamiya, R.; Ikeda, S. *J. Colloid Interface Sci.* **1985**, *108*, 215. (c) Lianos, P.; Zana, R. *J. Colloid Interface Sci.* **1981**, *84*, 100.
- (33) (a) Dorrance, R. C.; Hunter, T. F. *J. Chem. Soc., Faraday Trans. 1* **1972**, *68*, 1312. (b) Dorrance, R. C.; Hunter, T. F. *J. Chem. Soc., Faraday Trans. 1* **1974**, *70*, 1572.
- (34) (a) Turro, N. J.; Yekta, A. *J. Am. Chem. Soc.* **1978**, *100*, 5951. (b) Coll, H. *J. Phys. Chem.* **1970**, *74*, 520. (c) Granath, K. *Acta Chem. Scand.* **1953**, *7*, 297.
- (35) (a) Tanimoto, Y.; Itoh, M. *Chem. Phys. Lett.* **1981**, *83*, 626. (b) Tanimoto, Y.; Udagawa, H.; Katsuda, Y.; Itoh, M. *J. Phys. Chem.* **1983**, *87*, 3976. (c) Fendler, J. H.; Fendler, E. J.; Infantge, G. A.; Shih, P. S.; Patterson, L. K. *J. Am. Chem. Soc.* **1975**, *97*, 89.
- (36) (a) Sarpal, R. S.; Dogra, K. *J. Chem. Soc., Faraday Trans.* **1992**, *88*, 2725. (b) Hirose, C.; Sepulveda, L. *J. Phys. Chem.* **1981**, *85*, 3689.
- (37) Stigter, B. D.; Williams, R. J.; Mysels, K. J. *J. Phys. Chem.* **1955**, *59*, 330.